Technical Paper
J. Astron. Space Sci. 33(2), 137-146 (2016)
http://dx.doi.org/10.5140/JASS.2016.33.2.137

JASS Journal of Astronomy and Space Sciences

Correlation Between the "seeing FWHM" of Satellite Optical Observations and Meteorological Data at the OWL-Net Station, Mongolia

Young-Ho Bae[1†], Jung Hyun Jo[1,2], Hong-Suh Yim[1], Young-Sik Park[1], Sun-Youp Park[1], Hong Kyu Moon[1], Young-Jun Choi[1], Hyun-Jung Jang[1], Dong-Goo Roh[1], Jin Choi[1,2], Maru Park[1], Sungki Cho[1,2], Myung-Jin Kim[1], Eun-Jung Choi[1], Jang-Hyun Park[1]

[1]Korea Astronomy and Space Science Institute, Daejeon 34055, Korea
[2]University of Science and Technology, Daejeon 34113, Korea

The correlation between meteorological data collected at the optical wide-field patrol network (OWL-Net) Station No. 1 and the seeing of satellite optical observation data was analyzed. Meteorological data and satellite optical observation data from June 2014 to November 2015 were analyzed. The analyzed meteorological data were the outdoor air temperature, relative humidity, wind speed, and cloud index data, and the analyzed satellite optical observation data were the seeing full-width at half-maximum (FWHM) data. The annual meteorological pattern for Mongolia was analyzed by collecting meteorological data over four seasons, with data collection beginning after the installation and initial set-up of the OWL-Net Station No. 1 in Mongolia. A comparison of the meteorological data and the seeing of the satellite optical observation data showed that the seeing degrades as the wind strength increases and as the cloud cover decreases. This finding is explained by the bias effect, which is caused by the fact that the number of images taken on the less cloudy days was relatively small. The seeing FWHM showed no clear correlation with either temperature or relative humidity.

Keywords: meteorological data, cloud index, seeing, Mongolia, Space Situational Awareness, optical observations, wide field

1. INTRODUCTION

The OWL-Net Station No. 1 was installed as part of the Korea Astronomy and Space Science Institute's optical wide-field patrol (OWL) project. The station is an unmanned automatic station for the tracking of Korean satellites, and was set up at the Songino site of the Institute of Astrophysics and Geophysics (IAG) of Mongolia in May 2014. The site is located at 106° 20′ 5″ E, 47° 53′ 10″ N, which is about 50 km west of Ulaanbaatar, the capital of Mongolia, at an altitude of 1,674 m above sea level.

The meteorological conditions at a station are important factors for the future operation of the observation system at the station, because they affect the schedule and efficiency of observations, as well as the quality of acquired images. Moreover, the automatic observation systems used at unmanned stations such as the OWL-Net station are sensitive to the meteorological conditions because the system needs to be protected from external meteorological events.

Since the installation and beginning of test observation at the OWL-Net Station No. 1 in Mongolia in May 2014, more than a year's worth of meteorological data has been collected. The collected meteorological data were therefore analyzed to aid the efficient future operation of the station's observation system. The analytical data will be used to prepare an

Received May 13, 2016 **Revised** May 31, 2016 **Accepted** June 1, 2016
†**Corresponding Author**
E-mail: yhbae@kasi.re.kr, ORCID: 0000-0002-2738-6623
Tel: +82-42-865-2012, Fax: +82-42-865-3358

operation plan for the OWL-Net Station No. 1 and to inform preliminary studies on local meteorological data analysis by other research institutes that plan to install and operate observation stations in Mongolia.

In addition to the analysis of the seasonal and temporal trends of the meteorological data, the correlation between the meteorological conditions of Mongolia and the quality of the satellite optical observation images was analyzed. In this analysis, the data collected from the temperature, humidity, wind speed, and cloud sensors installed at the OWL-Net Station were used. Among these meteorological data, relative humidity and wind speed are closely related to the operation of the observation system and the quality of the satellite optical observation images, because the operation of the station can be limited by a high cloud index and the high probability of rain when the relative humidity is high. In addition, when the relative humidity is high, the atmospheric transparency can be low, causing scattering and absorption, and thus the brightness of the sky background can be high. A high wind speed may cause irregular physical loading on the telescope mount which supports optical tube, causing irregular errors during the pointing and tracking of a specific observation target, which may significantly affect the quality of the satellite optical observation images (Bradely et al. 2006). Generally, the quality of optical observation images such as those from satellites is represented by seeing, which is expressed as the full-width at half-maximum (FWHM) of the stellar images included in the optical observation images. Bradely et al. (2006) investigated the correlation between the Fried parameter, r_0, and the meteorological conditions on the ground near the summit of Mt. Haleakala, Hawaii, and reported that the parameter r_0 can be expressed as a function of wind speed and that the seeing worsens as the wind speed increases. On the other hand, Lombardi et al. (2007) analyzed meteorological data acquired at telescopio nazionale Galileo (TNG) and concluded that the seeing is optimal for wind speeds ranging from approximately 3.3 m/s to approximately 12 m/s, even compared with completely calm conditions.

As described above, previous studies indicated that the seeing is more closely correlated with wind properties, including wind direction and wind speed, than with the temperature and relative humidity. In this study, the local meteorological data accumulated over more than one year at the OWL-Net Station No. 1 in Mongolia were analyzed, and the correlation with the quality of the satellite optical observation images was quantitatively analyzed.

2. INSTRUMENTATION AT THE OWL-NET STATION, MONGOLIA

2.1 Meteorological Equipment

The OWL-Net Station No. 1 (Mongolia) has a number of meteorological sensors outside the station building, inside the dome, and inside the control room. Table 1 shows the location, type, and number of the installed meteorological sensors. The meteorological sensors installed inside the control room and the dome are used to investigate the internal status of each space. The meteorological sensors outside the station are installed at separate locations on the parapet of the station building. The diagram in Fig. 1 shows the locations of the meteorological sensors, and Fig. 2 shows a photograph of the installed meteorological sensors. The automatic weather station and the temperature and humidity sensor have the following model designations: WXT520 and HMT333 (VAISALA), respectively. The model designation of the cloud sensor is Boltwood Cloud Sensor Ⅱ (Diffraction Limited). The WXT520 sensor can measure the outdoor air temperature, relative humidity, wind direction, wind speed, and atmospheric pressure, while the

Table 1. Location of installation and quantities of the meteorological sensors at the OWL-Net Station (Mongolia)

Location	Sensor	Quantity
Outside of Station	Automatic Weather Station	1
	Temperature and Humidity Sensor	3
	Cloud Sensor	1
Inside Dome	Temperature and Humidity Sensor	1
Inside Control Room	Temperature and Humidity Sensor	1

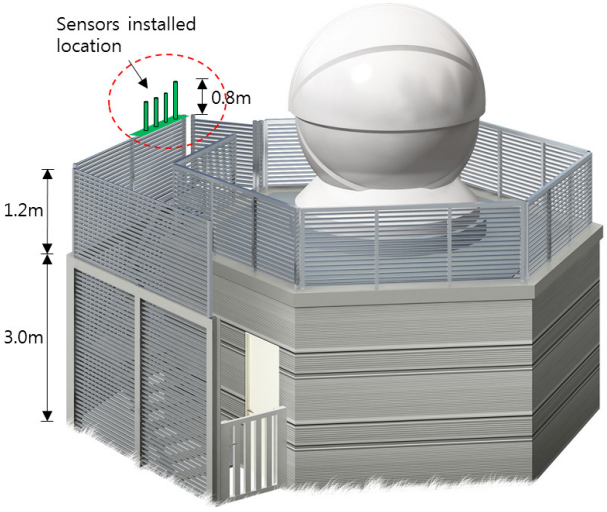

Fig. 1. Location of the installed meteorological sensors outside the station (inside the red dotted circle). Source: Concept design of the OWL-Net Station).

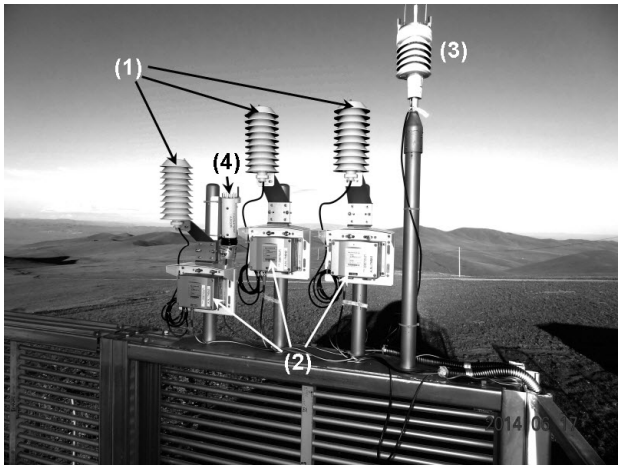

Fig. 2. Meteorological sensors on the OWL-Net No. 1 Station in Mongolia. (1) Solar shields for part of the sensors; (2) transmitter for the sensors; (3) automatic weather station; (4) cloud sensor.

HMT333 sensor can measure the outdoor air temperature and relative humidity. The Boltwood Cloud Sensor Ⅱ can measure the amount of cloud in a designated direction. The WXT520 sensor uses ultrasonic waves to measure wind direction and wind speed and lacks moving parts, allowing data collection to continue during freezing conditions in winter. The Boltwood Cloud Sensor Ⅱ can measure the amount of cloud by measuring the radiant heat with an infrared sensor; the sensor does not require a complicated hardware system such as charge-coupled device (CCD) or the installation of various software programs for image analysis. Fig. 2 shows the meteorological sensors that have been installed and operated at the OWL-Net Station No. 1. The detailed specifications of the individual sensors are shown in Table 2.

Table 2. Specifications of the meteorological sensors and cloud sensor on the station ("VAISALA official documents. Refer http://www.vaisala.com/ for meteorological sensors and http://www.cyanogen.com/cloud_main.php for cloud sensor.")

Automatic Weather Sensor (WXT520)	Operating Temperature	Range	-52 ~ +60°C
	Wind Speed Temperature	Range	0 ~ 60 m/s
		Accuracy	±0.3 m/s or 3% @ 0 ~ 35 m/s ±5% @ 35 ~ 60 m/s
		Resolution	0.1 m/s
		Range	-52 ~ +60°C
		Resolution	±0.3°C @ +20°C
	Relative Humidity	Range	0 ~ 100%RH
		Accuracy	±3%RH @ 0 ~ 90%RH ±5%RH @ 90 ~ 100%RH
Temperature and Humidity Sensor (HMT333)	Operating Temperature Temperature	Range	-40 ~ +60°C (for transmitter)
		Range	-70 ~ +180°C (for probe)
		Accuracy	±0.2°C @ +20°C
	Relative Humidity	Range	0 ~ 100%RH
		Accuracy (@ +15 ~ 25°C)	±1.0%RH @ 0 ~ 90% ±1.7%RH @ 90 ~ 100%
Cloud Sensor (Boltwood)		Method	Infrared Emission
		Output	Cloud index

Table 3. Observation units at the OWL-Net No. 1 Station (Mongolia)

Mount	Manufacturer	Rainbow Inc. (South Korea)
	Type	Alt-Az
Optics	Manufacturer	Officina Stellare (Italy)
	Aperture	500 mm
	F ratio	3.8
Detector	Manufacturer	FLI
	Pixel Scale	0.9″/pix
	FOV	1.1° × 1.1°

2.2 Telescope and Detector

An alt-azimuth type mount, 500 mm reflective optics, and a CCD detector were installed for satellite optical observations at the OWL-Net Station No. 1. Table 3 shows the detailed specifications of the individual observation instruments (Park et al. 2015).

3. STRATEGY FOR DATA ACQUISITION AT THE OWL-NET STATION, MONGOLIA

3.1 Meteorological Data

All the meteorological data collected by the meteorological sensors installed outside and inside the OWL-Net Station No. 1 are periodically transported to the control board installed in the control room. The control board collects the meteorological data and periodically transports the latest data to the main telescope operating system, which in turn saves the data as a file for each day. Fig. 3 shows the data transport flow and data transfer periods between individual devices.

The main telescope operating system identifies the current meteorological state based on the meteorological data measured by the sensors outside the station and transported from the control board, and then decides whether to perform an observation. The data used to decide whether to implement an observation include the wind speed from the automatic weather station, the temperature and relative humidity data from the temperature and humidity sensor, and the cloud index from the cloud sensor.

3.2 Optical Observations of Satellites

The OWL-Net Station No. 1 usually observes Korean satellites. Observations are implemented according to the observation schedule, but the intervals between

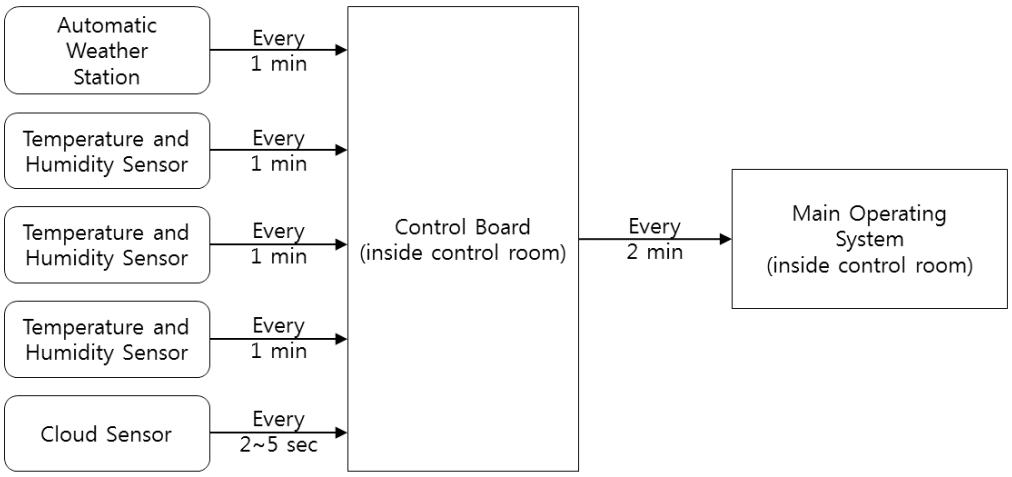

Fig. 3. Diagram for the data flow and the specific period for data transfers between devices. This figure shows the meteorological equipment installed outside the station only.

observations are not constant because of the need to find the optimum observation time for a target satellite. The exposure time was as short as 1 to 10 sec, because both end points of the satellite's trajectory should be included within the field of view of the optical system. Owing to the short exposure time and the brightness of the background sky, faint celestial bodies are rarely seen in the images, and thus the number of celestial bodies shown in each observation image is limited. However, the short exposure time means that the celestial bodies shown in an observation image are exposed to minimal meteorological changes, and thus the optical image of the celestial bodies reflects the momentary meteorological conditions.

Table 4. Operating period of the sensors and the number of observation days since June 2014

Year	Month	The number of operating day
2014	June	30
	July	29
	August	28
	September	28
	October	30
	November	29
	December	29
2015	January	30
	February	17
	March	31
	April	25
	May	22
	June	29
	July	27
	August	30
	September	8
	October	9
	November	30
Total	18 months	461 days

4. DATA ANALYSIS

4.1 Meteorological Data

The analyzed data were the meteorological data measured by the meteorological sensors installed outside the station, including a total of 18 months of data from June 2014 to November 2015, taken after the installation of the station and instruments and after the instrument stabilization test period. Table 4 shows the number of data collection days in each month. As can be seen in Table 4, the number of data collection days was relatively small in September and October 2015; this was because the normal operation of the station was suspended for a considerable period of time owing to an abnormality of the observation system.

The temperature and relative humidity data used for the data analysis were the least favorable values among the data measured by the three temperature and humidity sensors outside the station (i.e., the lowest of the three simultaneously acquired temperature values and the highest of the simultaneously acquired relative humidity values). This is an operational strategy of the unmanned automatic observation station as the main telescope operating system provides the criteria for the decision to start and discontinue observation. The raw wind speed and cloud data were employed since these two datasets were each collected from a single sensor.

According to Fig. 4, in Mongolia, at the location of the OWL-Net Station No. 1, the temperate remained below zero until May and remained above zero from June to August, gradually dropping below zero from September. The proportion of time for which the temperature was below

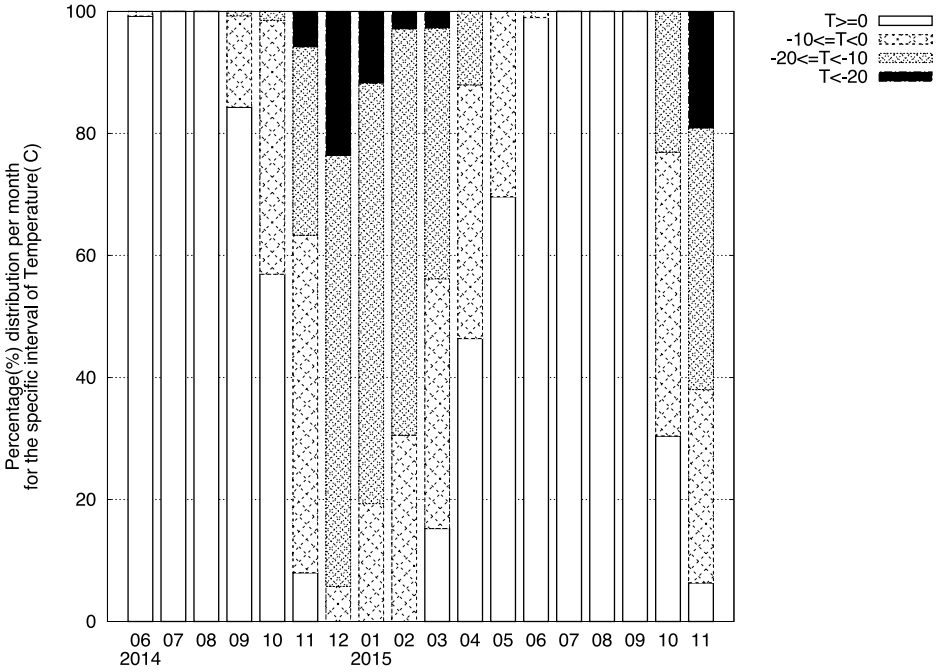

Fig. 4. Percentage distribution per month for specific temperature intervals.

zero drastically increased in October, and the temperature was below zero for the majority of each day in November. Harsh cold conditions with temperatures below –20℃ were sometimes observed in November, while the proportion of harsh cold days was about 23% or greater in December. The harsh cold weather continued until March, although the proportion of harsh cold days may have been lower. The lowest temperature measured during the observation period was approximately –27.9℃ at 23:00 on January 25, 2015, while the highest temperature was approximately 28.3℃ at 14:00 on August 10, 2015. During the observation period, temperatures above zero were observed about 47.7% of the time, and temperatures below zero were observed about 52.6% of the time, indicating similar proportions.

According to Fig. 5, the relative humidity was lower than 60% RH for about half of each month during the observation period. Relative humidities over 90% RH were predominantly found in summer, but these high humidity levels were observed for about 20% of the summer. The proportion of days when the relative humidity was over 90% RH was extremely small in winter.

Fig. 6 shows the monthly percentage distribution for individual wind speed intervals measured during the observation period. For more than half of the period, the wind was relatively weak with wind speeds < 5 m/s. Relatively strong wind speeds of 5 to 10 m/s were seen for about 2%, of the period, indicating that almost no strong wind occurred that might have affected the observations at the OWL-Net Station No. 1 in Mongolia during the observation period. The maximum wind speed, 20.2 m/s, was measured between 19:00 and 22:00 on April 14, 2015.

Fig. 7 shows the monthly percentage distribution of individual cloud index values measured during the observation period. The cloud index is the output of the cloud sensor, indicating the amount of cloud in the sky. The index expresses the difference between the radiant temperature of the sky and the ground temperature, as measured by the sensors. The cloud index usually has a negative value, with a value closer to zero indicating greater amounts of cloud and more negative values indicating less cloud cover. The cloud sensor is fixed in one direction, but the sensor can monitor a sufficiently broad section of sky for radiation, in the range of a solid angle of 80°.

The OWL-Net Station decides that an observation is possible if the cloud index is smaller than –30 or –50. The limiting value was empirically determined during the test observation period after the installation of the station. Therefore, analyzing Fig. 7 with reference to this value, very clear days (cloud index < –70) are usually observed in winter. The proportion of very clear days in a month was about 17% in January, 2015, while the proportion was much lower in other months. The proportion of days meeting the above cloud index condition for observation (cloud index < –50) was high in winter, at approximately 74% between December, 2014 and January, 2015.

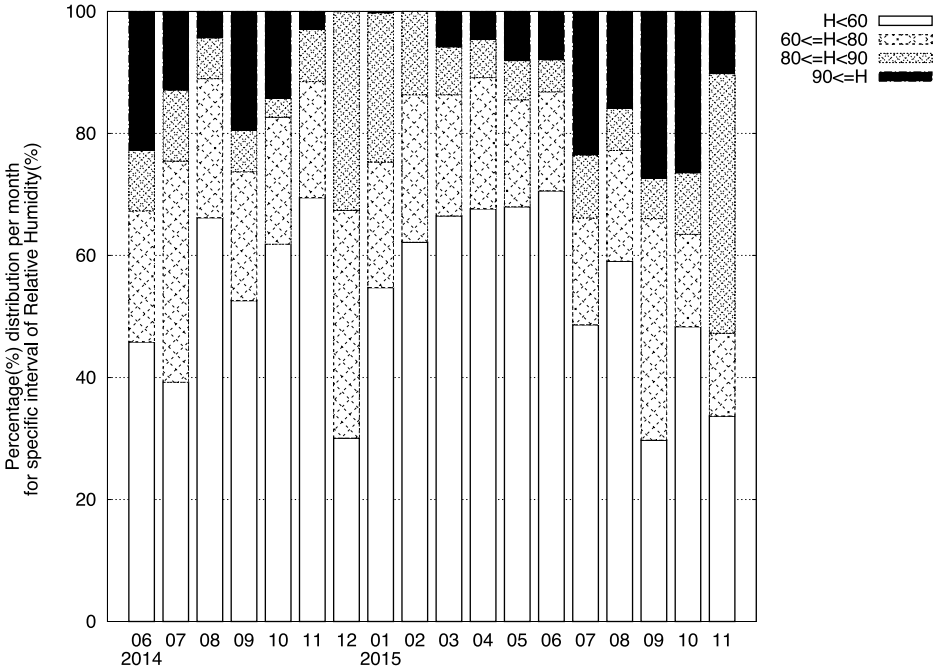

Fig. 5. Percentage distribution per month for specific relative humidity intervals.

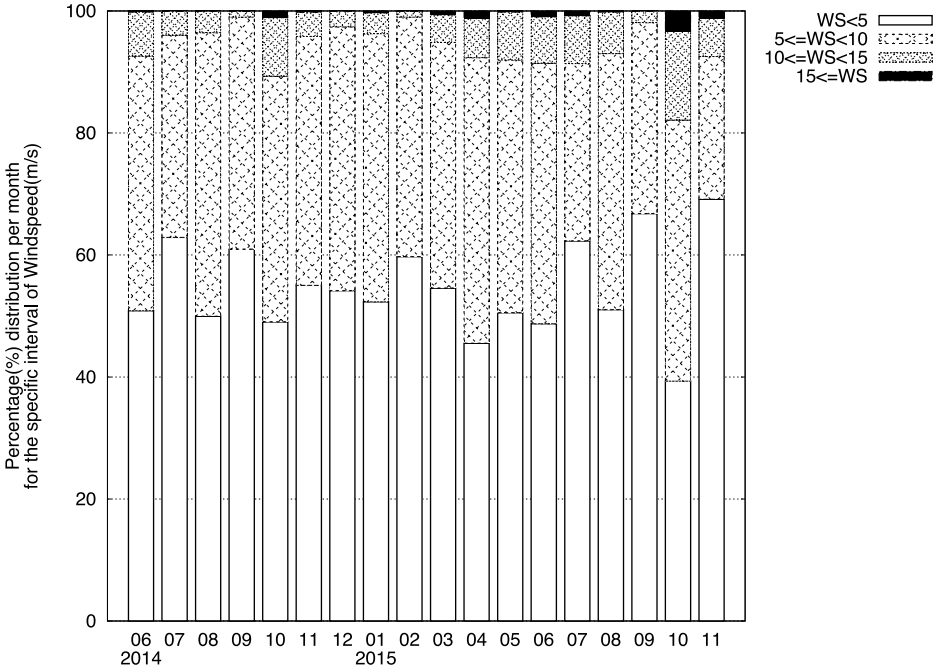

Fig. 6. Percentage distribution per month for specific wind speed intervals.

4.2 Full-Width at Half-Maximum Estimation for the Optical Observation of Satellites

To verify the correlation between the quality of the satellite optical observation images taken at the OWL-Net Station in Mongolia and the meteorological state at the station site, the optical observation images for the period shown in Table 4 were investigated. The quality of satellite optical observation images is generally determined with reference to seeing, which is expressed as the FWHM. Therefore, photometry was performed using the previously acquired optical observation images.

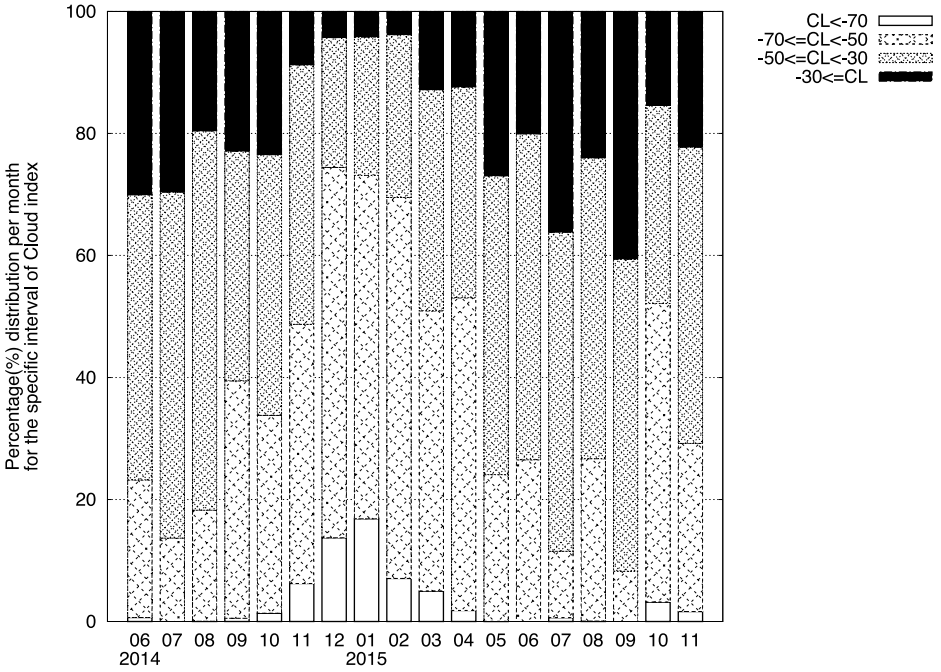

Fig. 7. Percentage distribution per month for specific cloud index intervals.

Fig. 8 shows a sample optical observation image from the OWL-Net Station in Mongolia. The indistinct dotted vertical line shows the trail of a satellite divided by the chopper like a electric fan. After photometry, the dotted trail was filtered to distinguish isolated star-like objects. Position information only was applied using the imexamine task in IRAF to find appropriate FWHM values for these objects.

"Source Extractor" (Bertin & Arnouts 1996; Bertin 2006) which is a program that photometry objects from an astronomical image and the imexamine task in IRAF were employed for the photometry of the optical observation images and the calculation of the FWHM. "Source Extractor" enables rapid photometry performance with many and large optical observation images.

Fig. 9 shows the scheme used to calculate representative FWHM values for the optical images. The details of the procedure are as follows:

1) "Source Extractor" was used to acquire the positions of any star-like objects included in one optical observation image.

2) The positions of the star-like objects were input into the "imexamine" task to calculate the FWHM.

3) "Imexamine" gives three types of FWHM values for each of the star-like objects included in one optical observation image: one is obtained directly using the photometric information, and the other two are obtained by calculating corrected FWHM values based on the directly calculated FWHM value.

4) The average of the three FWHM values was calculated for each object.

5) The average FWHM values of all the individual objects from a given image were once again averaged to obtain a representative FWHM value for one optical observation image.

Fig. 8. An optical image of a satellite trajectory taken by the OWL-Net Station in Mongolia. The indistinct dotted line shows a satellite trajectory by a chopper like a electric fan.

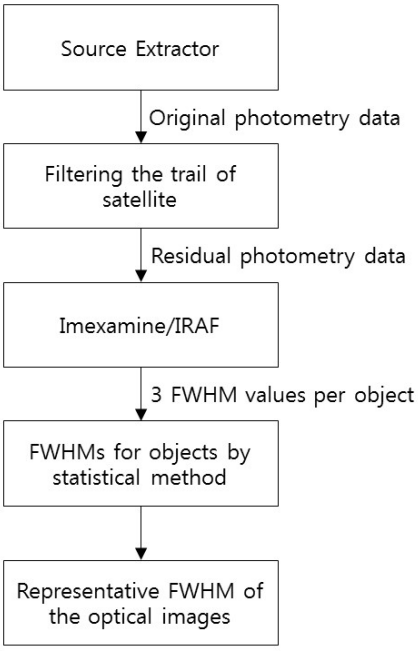

Fig. 9. Diagram for representative FWHM values for the optical images.

To obtain the meteorological data at the time when the individual optical observation images were taken, the temporal information for the two types of data were compared. Although the meteorological data were consecutively recorded every two minutes, the satellite observations were obtained at arbitrary times. Therefore, the temporal information included for the two types of data was not accurately synchronized, and the meteorological observations were made much more frequently than the satellite observations. Hence, if the elapsed time between the capture of a given optical observation image and the nearest meteorological data measurement was less than one minute, the meteorological data taken at the moment giving the smallest the time gap was considered as the meteorological data corresponding to the optical observation image. Therefore, the maximum time gap between the capture of an optical observation image and the measurement of the corresponding meteorological data was determined to be less than one minute. Although the total number of optical observation images acquired during the period was 6,758, the number of optical observation images for which meteorological data obtained at the corresponding time were available was smaller than this total number.

Fig. 10 shows the distribution of the representative FWHM values for the optical observation images. A comparative analysis of the representative FWHM values with the individual types of meteorological data will be described in the next section.

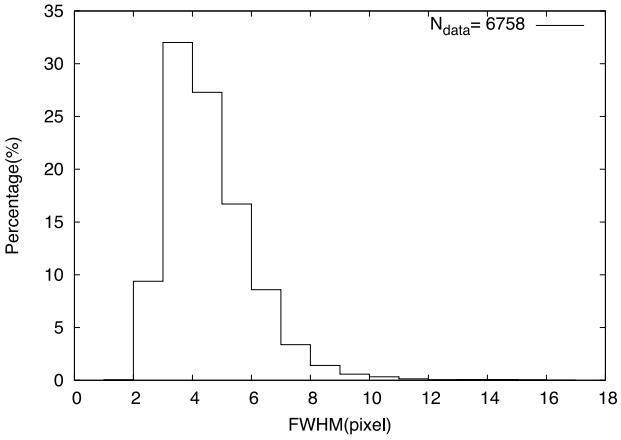

Fig. 10. A histogram of the representative FWHM distribution for each image.

5. CORRELATION BETWEEN THE FULL-WIDTH AT HALF-MAXIMUM OF ASTRONOMICAL OBJECTS AND METEOROLOGICAL DATA

Fig. 11 shows the correlations between the representative FWHM values for the individual optical observation images, and temperature and relative humidity. The upper section of the figure shows the correlation with temperature, while the lower section shows the correlation with relative humidity.

As shown in Fig. 11, the FWHM value does not correlate with either temperature or relative humidity. The only trend found is that the minimum FWHM value occurs when the outdoor air temperature was c. 5℃. The FWHM value gradually increased as the temperature moved above or below 5℃. However, this trend may be due to differences in the imaging frequency between the intervals. Similarly, a weak correlation may be found in the case of relative humidity and for the temperature distribution, but these correlations may also be due to the imaging frequency differences.

In conclusion, as can be seen in Fig. 11, the FWHM value obtained at the OWL-Net Station in Mongolia did not show a definite correlation with temperature or relative humidity.

Fig. 12 shows the correlation between the representative FWHM values for the individual optical observation images and the cloud index.

Generally, considering only the cloud index, it is presumed that the FWHM value of the optical observation images may decrease as the amount of cloud decreases (i.e., as the cloud index becomes more negative). However, as shown in Fig. 12, the FWHM value increased as the

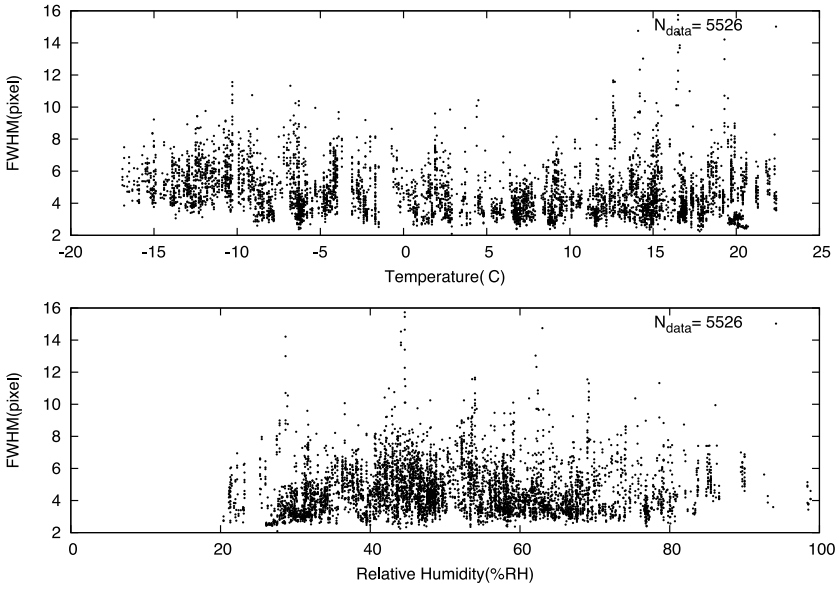

Fig. 11. Representative FWHM values vs. temperature and relative humidity.

amount of cloud decreased. As in the cases of temperature and relative humidity, this may be due to differences in the imaging frequency. A comparison of the trend with Fig. 6 may elucidate the reason. As shown in Fig. 6, approximately 10% of the entire analysis period saw a cloud index value < –70. Even though only the nighttime coinciding with the observation is taken into consideration, the ratio may be similar. Therefore, the result indicates that the number of days with very clear skies may be small at the station site given the weather conditions of Mongolia. Hence, the possibility of obtaining images with a very clear sky may be low, and the FWHM value therefore seems to be greater when the sky is clearer, as shown in Fig. 12.

If there were enough images taken when the cloud index was less than –70, which would indicate that there was almost no cloud, a trend of decreasing FWHM values with decreasing cloud cover might have been expected. However, this trend cannot be verified with the current data alone.

Fig. 13 shows the correlation between the FWHM value and wind speed. The solid red line is the approximate trend obtained by the least squares method for the two datasets.

According to Fig. 13, the overall FWHM is positively correlated with wind speed. In other words, when the FWHM is greater, the wind speed is also greater. This indicates that wind speed has a closer correlation with the FWHM than other meteorological data such as temperature and relative humidity. The solid red line in Fig. 13 represents the approximate trend line for the FWHM and wind speed. The equation for this line is

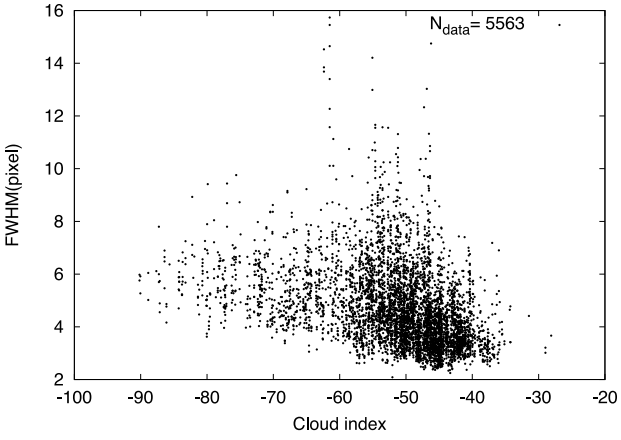

Fig. 12. Representative FWHM values vs. cloud index.

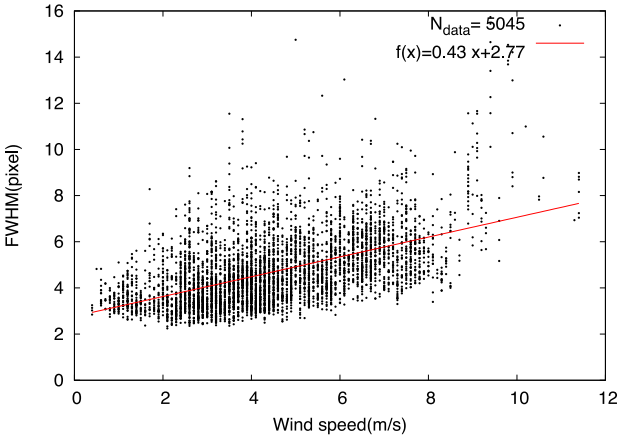

Fig. 13. Representative FWHM values vs. wind speed. The red solid line represents the fitted line for the datasets.

$$f(x) = 0.43 \times x + 2.77 \quad (1)$$

where x denotes wind speed (m/s), and $f(x)$ the FWHM (pixel). According to this expression, the best FWHM obtainable from the OWL-Net Station, under meteorological conditions without wind, should be approximately 2.77 pixels.

6. RESULTS AND SUMMARY

Meteorological data collected at the OWL-Net Station No. 1 (Mongolia), installed in 2014, over a period of 18 months from June 2014 to November 2015 were analyzed, and a correlation between the meteorological data and the seeing of the satellite optical observation data collected during the same period was analyzed. Among the meteorological data, temperature, relative humidity, wind speed, and cloud index were analyzed. The temperature and relative humidity data used for the data analysis were the least favorable values among the data measured simultaneously by three identical devices. The raw wind speed and cloud datasets, each collected by a single sensor, were used for the data analysis.

The analysis of the meteorological data showed that temperatures below zero first occurred in September and continued until the following May at the OWL-Net Station site in Mongolia. The harsh cold period, with temperatures below –20℃, when observations were not carried out, began in early November and continued until late March in the next year.

Highly humid environments, with 80% RH or higher, were primarily observed in summer, but the proportion of days in a month seeing these high humidity values was less than 30%. Highly humid environments, with 90% RH or higher, when observations were not made, were also primarily seen in summer and rarely found in winter.

The outdoor air temperature, relative humidity, wind speed, and cloud index were compared with the FWHM of the optical observation images. The results showed that the FWHM is not correlated with outdoor air temperature or relative humidity. A comparison of the FWHM with the cloud index showed that the FWHM value increased as the cloud index became more negative, that is, as the amount of cloud decreased. The biggest contribution to this result may be the bias effect caused by the fact that the number of images taken on relatively cloudless days was extremely small. Many other meteorological conditions may also have affected the result. To verify the effects of the meteorological conditions, more optical observation images taken on relatively cloudless days are needed.

Wind speed has a stronger correlation with the FWHM value than other data. As the wind speed increased, the FWHM value was worse, which is consistent with previous studies. However, the opposite result was found in a study by Lambardi et al. (2007), who obtained an optimum FWHM for a certain range of wind speeds. Therefore, meteorological data obtained over a longer period than that of the data used in this study may be required for analysis.

ACKNOWLEDGMENTS

This work was supported by the National Agenda Project "Development of Electro-optic Space Surveillance System" funded by Korea Research Council of Fundamental Science & Technology (KRCF) and the Korean Astronomy and Space Science Institute (KASI).

REFERENCES

Bertin E, Arnouts S, SExtractor: Software for source extraction, Astron. Astrophys. Suppl. Ser. 117, 393-404 (1996). http://dx.doi.org/10.1051/aas:1996164

Bradely ES, Roberts LC, Bradford LW, Skinner MA, Nahrstedt DA, et al., Characterization of meteorological and seeing conditions at Haleakala, Publ. Astron. Soc. Pac. 118, 172-182 (2006). http://dx.doi.org/10.1086.497622

Lombardi G, Zitelli V, Ortolani S, Pedani M, El Roque de Los Muchachos site characteristics. II. Analysis of wind, relative humidity, and air pressure, Publ. Astron. Soc. Pac. 119, 292-302 (2007). http://dx.doi.org/10.1086/513079

Park S, Choi J, Jo JH, Son JY, Park YS, et al., Development of a reduction algorithm of GEO satellite optical observation data for Optical Wide field patroL (OWL), J. Astron. Space Sci. 32, 201-207 (2015). http://dx.doi.org/10.5140/JASS.2015.32.3.201